Interaction and Stimulation of Human FEN-1 Nuclease Activities by Heterogeneous Nuclear Ribonucleoprotein A1 in α-Segment Processing during Okazaki Fragment Maturation†

Qing Chai,‡,⊥ Li Zheng,‡,⊥ Mian Zhou,‡ John J. Turchi,§ and Binghui Shen*,‡

Division of Molecular Biology, City of Hope National Medical Center and Beckman Research Institute, Duarte, California 91010, and Department of Biochemistry and Molecular Biology, Wright State University School of Medicine, Dayton, Ohio 45435

Received August 1, 2003; Revised Manuscript Received October 23, 2003

ABSTRACT: High-fidelity DNA replication depends on both accurate incorporation of nucleotides in the newly synthesized strand and the maturation of Okazaki fragments. In eukaryotic cells, the latter is accomplished by a series of coordinated actions of a set of structure-specific nucleases, which, with the assistance of accessory proteins, recognize branched RNA/DNA configurations. In the current model of Okazaki fragment maturation, displacement of a 27-nucleotide or longer flap is envisioned to attract replication protein A (RPA), which inhibits flap endonuclease-1 (FEN-1) but stimulates Dna2 nuclease for cleavage. Dna2 cleavage generates a short flap of 5−7 nucleotides, which resists binding by RPA and further cleavage by Dna2. FEN-1 then removes the remaining flap to produce a suitable substrate for ligation. However, FEN-1 is not efficient in cleaving the short flap, and we therefore set out to identify cellular factors that might regulate FEN-1 activity. Through co-immunoprecipitation experiments, we have isolated heterogeneous nuclear ribonucleoprotein A1 (hnRNP A1), which forms a direct complex with FEN-1 and stimulates its enzymatic activities. The stimulation by hnRNP A1 is most dramatic using DNA substrates with short flaps. With longer flap substrates the hnRNP A1 effect is more modest and is suppressed by the addition of RPA. A model is provided to explain the possible in vivo role of this interaction and activity in Okazaki fragment maturation.

Okazaki fragments are formed during DNA lagging strand synthesis. This process is initiated by DNA polymerase α, which synthesizes a short RNA−DNA primer. We term this RNA−DNA primer the α-segment. The α-segment is then elongated by DNA polymerase δ to make a nascent lagging strand DNA of about 200 nucleotides in length. These nascent DNA segments or Okazaki fragments are processed by nucleases, DNA polymerases, and DNA ligases to complete the DNA lagging strand duplication (*1*−*4*). Nucleases play a crucial role in maturation of Okazaki fragments. At first sight, the processing of Okazaki fragments might appear to require that only the short RNA segment be removed and replaced with DNA. However, DNA polymerase α lacks a proofreading function. The short stretch of Pol α-synthesized DNA fragment adjacent to the RNA primer must be removed as this may contain highly mutagenic misincorporated bases.

RNase H and flap endonuclease 1 (FEN-1)[1] were first implicated to be required for RNA primer removal in eukaryotic in vitro reconstitution experiments (*4*−*7*). However, in yeast, deletion of individual genes encoding RNases H, which are possibly involved in RNA primer removal, or a combination of these null mutations does not result in an obvious phenotype (*6*, *8*). Deletion of the *RAD27* gene, a *Saccharomyces cerevisiae* FEN-1 homologue, reveals a temperature-sensitive lethality phenotype with formation of dumb-bell-shaped cells having a single nucleus. This terminal phenotype and information obtained from mutation spectrum analysis support the conclusion that null *rad27* is a replication-deficient mutant (*9*−*12*). Our more recent work demonstrated that double deletion of both *S. cerevisiae* RNase H(35), a major DNA replication RNase H, and Rad27 caused more severe phenotypes derived from DNA replication (*6*).

The fact that deletion of *RAD27* does not lead to lethality of yeast cells indicates that a backup pathway(s) for α-segment processing exists in yeast, which allows survival at the permissive temperature of 30 °C, but operates inefficiently at the nonpermissive temperature of 37 °C. One such enzyme is the *S. cerevisiae* Dna2. The enzyme was initially identified as a helicase, and later it was found to have single-stranded DNA/RNA endonuclease activity, which is suited for removing RNA primers of Okazaki fragments (*13*, *14*). Deletion of the *DNA2* gene is lethal in yeast (*14*).

† This work was supported by National Institutes of Health Grant CA085344 (B.S.).

* Author to whom correspondence should be addressed. Phone: (626) 301-8879. Fax: (626) 301-8280. E-mail: bshen@coh.org.

⊥ These authors contributed equally to this work.

‡ City of Hope National Medical Center and Beckman Research Institute.

§ Wright State University School of Medicine.

[1] Abbreviations: FEN-1, flap endonuclease-1; hnRNP A1, heterogeneous nuclear ribonucleoprotein A1; RPA, replication protein A; PCNA, proliferating cell nuclear antigen; APE-1, AP endonuclease; WRN, Werner's syndrome; NHEJ DNA repair, nonhomologous-end-joining DNA repair.

10.1021/bi035364t CCC: $25.00
Published on Web 12/03/2003

Dna2 interacts genetically and physically with several proteins involved in maturation of the Okazaki fragments, including FEN-1/Rad27 nuclease (*15*) and replication protein A (RPA; *16*, *17*). More recently, it has been shown that the endonucleases Dna2 and FEN-1 act sequentially to facilitate the maturation of Okazaki fragments (*13*, *17*, *18*). The sequential actions of these enzymes have been demonstrated to be governed by a single-stranded DNA binding protein, RPA (*16*). In this so-called "RPA-governed nuclease switch model" for Okazaki fragment processing, displacement of a flap of length greater than 27 nucleotides is envisioned to attract RPA, which inhibits FEN-1 but stimulates Dna2 for cleavage (*17*). The binding of RPA to the single-stranded RNA primer recruits Dna2 nuclease. The Dna2/RPA complex cleaves the major portion of the primer. This generates a short flap of approximately 5−7 nucleotides, which resists binding by RPA and cleavage by Dna2. FEN-1/Rad27 nuclease then removes the remaining flap to produce a substrate for ligation.

However, previous data indicated that the nuclease activity of FEN-1 is greatest when the single-stranded flap is about 20 nucleotides, and that cleavage efficiency falls dramatically if the single-stranded flap is shorter than 10 nucleotides (*19*, *20*). Therefore, if the sequential model is correct, the RNA primers of Okazaki fragments may not be efficiently removed without additional cofactors. Such a scenario led us to search for an FEN-1 interacting protein, which binds to the short single-stranded flap, forms a complex with FEN-1, and stimulates its enzyme activity. Through co-immunoprecipitation experiments, we have isolated heterogeneous nuclear ribonucleoprotein A1 (hnRNP A1), which has been reported to possess characteristics that we believe make it a good cofactor candidate. This protein not only binds to both RNA and single-stranded DNA (*21*−*23*), but in this work we demonstrate that it also forms a complex with FEN-1 during the S-phase of the cell cycle in cultured HeLa cells and can stimulate FEN-1 activities required for Okazaki fragment maturation. We provide an explanation for the physiological role of this interaction in α-segment processing during Okazaki fragment maturation.

EXPERIMENTAL PROCEDURES

Cell Culture and Immunoprecipitation. HeLa S3 cells were cultured in DMEM medium (Irvine Scientific, Santa Ana, CA), supplemented with 10% fetal calf serum, 2 mM glutamine, and 1% penicillin/streptomycin. HeLa S3 cells were synchronized at the G1/S boundary using 200 μM mimosine (Sigma, St. Lois, MO) according to a previously published procedure (*24*). Nuclear extracts were prepared as previously described (*24*) suspended in a binding buffer containing 50 mM Tris−Cl, pH 8.0, 0.1% NP-40, 150 mM NaCl, and protein inhibitor cocktails (Roche Molecular Biochemicals, Indianapolis, IN) and were incubated with the polyclonal anti-hFEN-1 antibody linked to protein A−agarose beads. Agarose beads were washed 3−6 times with the same binding buffer. Protein complexes were separated on 4−15% gradient SDS−PAGE (Bio-Rad, Hercules, CA) and analyzed by amino acid microsequencing (City of Hope, Duarte, CA) or detected by Western blot. Monoclonal antibody against hnRNP A1 was a kind gift from Dr. Gideon Dreyfuss. Polyclonal hnRNP A1 antibody was purchased from Santa Cruz Biotechnology, Inc., Santa Cruz, CA.

Protein Expression and Purification. To construct the expression vector of recombinant hnRNP A1 protein, a DNA fragment encoding human hnRNP A1 was amplified by RT-PCR using total RNA extracted from HeLa S3 cells with the Rneasy Mini Kit (Qiagen, Valencia, CA) as the template. The PCR product was subcloned into pGEX-4T vector (Pharmacia Biotech, Piscataway, NJ). DNA fragments encoding hnRNP A1 deletion mutants UP1 and the glycine-rich domain (GRD) were amplified using cDNA of hnRNP A1 as the template, and subcloned into pGEX-4T vector. All inserts were confirmed by DNA sequencing. Plasmids encoding GST−hnRNP A1, GST−UP1, or GST−GRD were transformed into *Escherichia coli* BL21. The transformants were grown at 37 °C overnight in 2XYT medium in the presence of ampicillin (50 μg/mL). Bacterial cultures were diluted with fresh 2XYT medium and incubated for 3 h at 30 °C. The cells were induced by 0.4 mM isopropyl thio-β-D-galactopyroanoside (Sigma) for 4 h, and then collected by centrifugation. Cell lysates were prepared by ultrasonication. Soluble GST fusion proteins were purified using glutathione−Sepharose affinity chromatography. Bound proteins were then eluted with a buffer containing 50 mM Tris−HCl, pH 8.0, and 15 mM glutathione. FEN-1 protein was purified in our laboratory previously (*25*). Endogenous human RPA was purified from HeLa cells using the three-column chromatography procedure previously described for the purification of recombinant RPA (*26*).

GST Pull-Down Assay. Purified GST fusion proteins were coupled to Sepharose beads and mixed with precleared bacterial crude extract expressing 6His-tagged hFEN-1. After a 3 h incubation at 4 °C on a rotating platform, the beads were collected by centrifugation at 1000*g* in microcentrifuge tubes. The beads were then washed three times with binding buffer (50 mM Tris−HCl, pH 8.0, 50 mM NaCl) and twice with washing buffer (50 mM Tris−HCl, pH 8.0, 1 M NaCl). Proteins bound to the beads were then analyzed by SDS−PAGE followed by Western blot using anti-hFEN-1 antibody.

Yeast Two-Hybrid Assays. Yeast two-hybrid analysis was performed with hnRNP A1 gene in the pACT2 (activation domain) vector and with FEN-1 gene in the pAS2-1 (DNA binding domain) vector (Clontech, Palo Alto, CA) and vice versa. Paired vectors were transformed into *S. cerevisiae* strain AH109 by the lithium acetate method according to the manufacturer's recommendation. Interaction in the two-hybrid system was tested by growth on histidine-deficient selective media with 5 mM 3-aminotriazole (3-AT) and 5-bromo-4-chloro-3-indolyl-α-galactopyranoside (X-α-Gal), and by β-galactosidase activity, which was determined by colony filter assay according to the manufacturer's instruction.

Preparation of DNA Substrates. The 5′ flap DNA substrate was prepared according to our published procedure (*25*). Oligonucleotide sequences used for DNA substrates are listed in Table 1. The primer−template substrate is specified in the figure caption in ref *25*. To label the 5′ end of DNA substrates, the oligonucleotide as specified in the figure caption was incubated with 20 μCi of [γ-^{32}P]ATP and 10 units of polynucleotide kinase at 37 °C for 30 min. To label the 3′ end of DNA substrates, the oligonucleotide was incubated with 20 μCi [α-^{32}P]ddATP and 10 units of terminal DNA transferase at 37 °C for 30 min. After inactivation of polynucleotide kinase or terminal DNA transferase by heating

Table 1: Oligonucleotides Used To Construct the Nuclease Substrates[a]

Flap Strands		
flap 20	34-mer	5′-*GATGTCAAGCAGTCCTAACT*TTGAGGCAGAGTCC-3′
flap 9	23-mer	5′-*GTCCTAACT*TTGAGGCAGAGTCC-3′
flap 1	15-mer	5′-*A*TTGAGGCAGAGTCC-3′
RNA flap	37-mer	5′-*gggaacaaaagcuugcaugccTG*CAGGTCGAC TCTAG-3′
Upperstream Strands		
Prim-3B1	16-mer	5′-CACGTTGACTACCGTC-3′
Prim-3B2	17-mer	5′-CACGTTGACTACCGTCC-3′
Template Strands		
Temp-G1	30-mer	5′-GGACTCTGCCTCAAGACGGTAGTCAA CGTG-3′
Temp-G2	30-mer	5′-CTAGAGTCGACCTGGACGGTAGTCAA CGTG-3′

[a] Italic letters indicate the unannealed flap portion. The lower-case letters represent the RNA portion of the oligonucleotide, while the upper-case letters represent the DNA portion.

the sample at 72 °C, the oligonucleotide was annealed with the corresponding primer and template oligonucleotides by incubation at 70 °C for 5 min followed by slow cooling to 30 °C. The DNA was then precipitated by addition of 20 μL of 3 M sodium acetate and 1 mL of absolute ethanol, followed by resuspension of the precipitate in water. For the DNA binding assay, the 5′ biotinylated Temp-G1 was annealed with unlabeled flap 9 and Prim-3B1 using the same annealing protocol.

FEN-1 Nuclease Activity Assay. The cleavage of DNA substrates by FEN-1 was determined by our previously published nuclease assay (*25*). In brief, ^{32}P-labeled DNA substrates were incubated with purified FEN-1 in a buffer solution containing 50 mM Tris−HCl, pH 8.0, 50 mM NaCl, and 5 mM $MgCl_2$. The reactions were carried out at 37 °C for 15 min, and were terminated with stop solution (95% formamide, 20 mM EDTA, 0.05% bromphenol blue, 0.05% xylene cyanol). The product and substrate were then separated by 15% denaturing polyacrylamide gel electrophoresis and visualized by autoradiography.

DNA Substrate Binding Assay. The DNA substrate binding ability was measured using a method similar to that published previously (*27*). The biotinylated DNA substrates were immobilized onto the Neutro-avidin agarose by incubating them in 10 mM Tris−Cl, pH 7.5, 1 mM EDTA, and 1 M NaCl at 25 °C for 2 h. The beads were washed twice with the same buffer solution used for the linking reaction and resuspended in a solution containing 30 mM Hepes−NaOH, pH 7.5, 125 mM NaCl, 0.2 mg/mL BSA, 1 mM dithiothreitol (DTT), and 5 mM Mg^{2+}. DNA-bound beads were incubated with 3 μM hFEN-1 in the presence of varying amounts of hnRNP A1 on ice for 1 h. The beads were then washed twice with a buffered solution (30 mM Hepes−NaOH, pH 7.5, 125 mM NaCl, 0.1 mg/mL BSA, 5% glycerol, 1 mM DTT, 0.01% NP-40, and 5 mM Mg^{2+}). The protein bound to the beads was separated by 4−15% gradient SDS−PAGE and detected by immunoblot using polyclonal anti-FEN-1 antibody as the first antibody.

RESULTS

hnRNP A1 Physically Interacts with hFEN-1. To purify proteins that complex with hFEN-1 during DNA replication, HeLa S3 cells were synchronized according to the published protocol (*24*) Nuclear extracts of S-phase cells were prepared and then incubated with protein A−agarose harboring anti-FEN-1 antibody. Proteins that co-immunoprecipitate with hFEN-1 were resolved on 4−15% gradient SDS−PAGE and analyzed with mass spectroscopy microsequencing (City of Hope, Duarte, CA). Several known and new peptides were identified from what was recovered in SDS−PAGE. PCNA was one of the proteins which were pulled down in our immunoprecipitation assay. It is known that PCNA interacts with FEN-1 and stimulates its activity significantly. A single-stranded RNA binding protein, hnRNP A1, was also identified from the hFEN-1 complex in the same experiment. To confirm that hnRNP A1 is coprecipitated with hFEN-1, proteins pulled down with FEN-1 during the S-phase were analyzed by SDS−PAGE followed by immunoblotting using anti-hnRNP A1 antibody. The results revealed that hnRNP A1 was pulled down with hFEN-1 by anti-FEN-1 antibody, but not with control antibodies (Figure 1A). It is known that hnRNP A1 interacts with both RNA and single-stranded DNA with considerable affinity and that hFEN-1 can also bind to a single-stranded flap DNA substrate. It is possible that hnRNP A1 or hFEN-1 might be brought down indirectly through their individual interaction with nucleic acids present in cell extracts. To investigate this possibility, cell lysates were pretreated with micrococcal nuclease (MCN), which can effectively digest nucleic acids. Our results showed that MCN treatment did not affect the coprecipitation of hnRNP A1 and hFEN-1, indicating that the interaction between

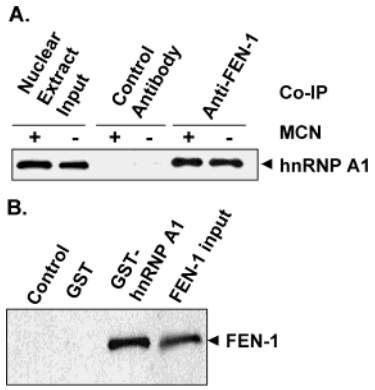

FIGURE 1: hnRNP A1 physically interacts with FEN-1. (A) Co-immunoprecipitation of HeLa S3 cells by anti-FEN-1 antibody. HeLa cell nuclear extracts (3 mg/mL) were incubated with anti-FEN-1 or control antibody coupled to protein A beads in the absence or presence of micrococcal nuclease. hnRNP A1 bound to agarose was detected by anti-hnRNP A1 antibody. (B) GST pull-down assay. GST−hnRNP A1 was purified with GSH−agarose. The crude extract of bacterial cells expressing 6His−FEN-1 was incubated with GST−hnRNP A1-bound agarose. After extensive washing, hnRNP A1-bound FEN-1 was detected with anti-FEN-1 antibody. FEN-1 input was loaded with 1/50 of the crude extract for the pull-down assay. Agarose beads and GST−agarose beads were used as negative controls.

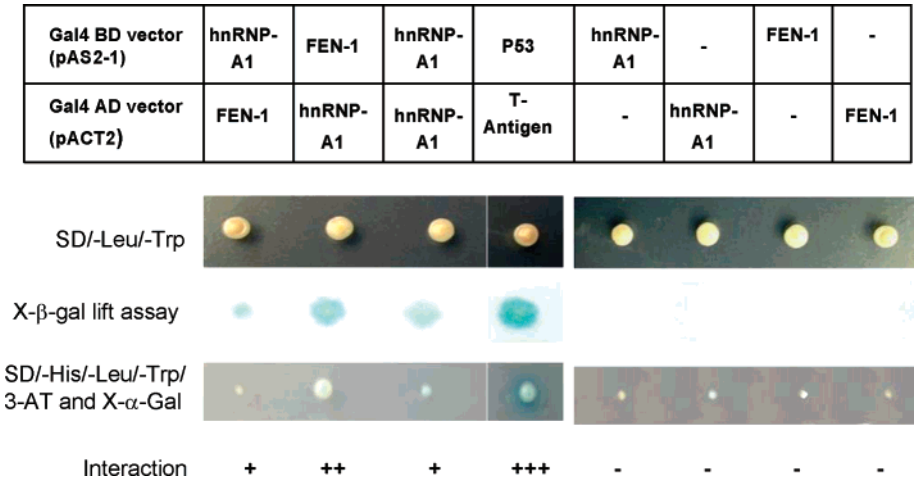

FIGURE 2: FEN-1 and hnRNP A1 interaction assayed in vivo by the yeast two-hybrid system. pAS2 and pACT2 are plasmid vectors encoding the Gal4 DNA binding domain (BD) and transcriptional activation domain (AD), respectively. Paired constructs were grown on SD medium without Trp and Leu. Transformants were assayed for β-galactosidase activity by both filter assay and liquid assay (data not shown). Blue colonies indicate interaction. Protein interaction was also determined by blue colonies grown on an SD/His/Leu/Trp selection plate with 5 mM 3-AT and X-α-Gal. The interaction between murine p53 and SV40 large T antigen is used as a positive control. The interaction is scored with plus and minus signs. The minus sign represents no interaction, while the plus sign represents positive interaction.

hnRNP A1 and hFEN-1 is direct and nucleic acid independent (Figure 1A).

To further confirm the physical interaction between hnRNP A1 and hFEN-1, hnRNP A1 was expressed as a GST-fusion protein, and hFEN-1 was expressed with a 6His tag. The interaction between these two proteins was then determined by a GST pull-down assay. The results indicated that significant interaction occurred between hFEN-1 and hnRNP A1 and this interaction was specific for hnRNP A1, because neither empty agarose nor GST-bound agarose can bind to hFEN-1 (Figure 1B). Additionally, no protein from cell lysates of *E. coli* harboring an empty pET28b plasmid was pulled down by GST or GST−hnRNP A1 (data not shown).

To validate the in vitro results of the interaction between hnRNP A1 and hFEN-1, we used the yeast two-hybrid system. cDNAs encoding hnRNP A1 and hFEN-1 proteins were independently cloned into pAS2-1 and pACT2 vectors to express hnRNP A1 or FEN-1 as a fusion protein to the GAL4 DNA binding domain (BD) or as a fusion protein to the GAL4 activation domain (AD). Upon cotransformation with pairs of fusion proteins, the cotransformants were preselected with SD/-Leu/-Trp plates. The interaction was evaluated by SD/-His/-Leu/-Trp selection and by β-galactosidase activity. The results revealed that yeast coexpressing BD-fused hnRNP A1 and AD-fused hFEN-1 or BD-fused hFEN-1 and AD-fused hnRNP A1 could well grow on the SD/His/Leu/Trp with 3-AT and X-α-Gal plate (Figure 2). The coexpression of these reversed pairs considerably induced the expression of β-galactosidase, albeit to a lesser extent than did the positive control (coexpression of BD-fused P53 and AD-fused T-antigen) (Figure 2). We noticed an orientation-dependent interaction; that is, BD-fused FEN-1 and AD-fused hnRNP A1 have stronger interaction than their reciprocal pair of fusion proteins. Possibly, the DNA-BD/FEN-1 fusion protein has better nuclear localization and/or recognition of the GAL1 UAS region. BD-fused hnRNP A1 or AD-fused hFEN-1 alone cannot induce β-galactosidase expression. Self-interaction of hnRNP A1 (A1−A1) was previously reported (*28*).

hnRNP A1 Stimulates hFEN-1 Nuclease Activities. We evaluated the effects of hnRNP A1 on FEN-1-catalyzed cleavage of DNA substrates with varying lengths of 5′ flap structure. Three flap DNA substrates were used in this study, flap 20, flap 9, and flap 1, which have a flap of 20, 9, and 1 nucleotide(s) in length, respectively. Our results indicated that hnRNP A1 could stimulate hFEN-1 to cleave all three DNA substrates. However, the stimulation of hFEN-1 to cleave flap 9 or flap 1 was approximately 20-fold, while the stimulation of hFEN-1 to cleave the flap 20 substrate was about 3-fold (Figure 3). In control experiments, BSA and GST were shown to have no effect on the hFEN-1 nuclease activity. The effect of RPA on FEN-1 nuclease activity produced varied results. Initially, RPA was shown to stimulate FEN-1 nuclease activity (*29*). More recently, RPA has been shown to inhibit FEN-1 cleavage activity of DNA substrate with a 20-nucleotide or longer flap (*16*). In our assay, RPA completely suppressed FEN-1-catalyzed cleavage of the flap 20 substrate, and hnRNP A1 was unable to reverse this inhibitory effect (Figure 3A). However, RPA significantly stimulated hFEN-1 cleavage of flap 9 and flap 1 DNA substrates. Interestingly, the stimulation of FEN-1 activity by RPA and hnRNP A1 was additive on these shorter DNA substrates (Figure 3B,C). We next examined the effects of hnRNP A1 on FEN-1 cleavage of DNA substrates with a double-flap structure, which recently has been suggested to be a cellular substrate of FEN-1 (*30*). Our results revealed that, compared with the corresponding single-flap substrates, FEN-1 is significantly more active in cleaving the double-flap substrate (Figure 3B,D). However, hnRNPA1, RPA, or the combination of the two proteins did not enhance the cleavage of double-flap DNA substrates by FEN-1 (Figure 3D). The fact that hnRNP A1 does not stimulate the double-flap-substrate-based FEN-1 nuclease activity may indicate that the 3′ flap and hnRNP A1 mediate the FEN-1 protein conformational changes to an optimal status for nuclease activity in a similar manner.

hnRNP A1 Enhances DNA Dubstrate Binding and Catalysis by hFEN-1. Having demonstrated that hnRNP A1 can directly bind to FEN-1 and stimulate its nuclease activity,

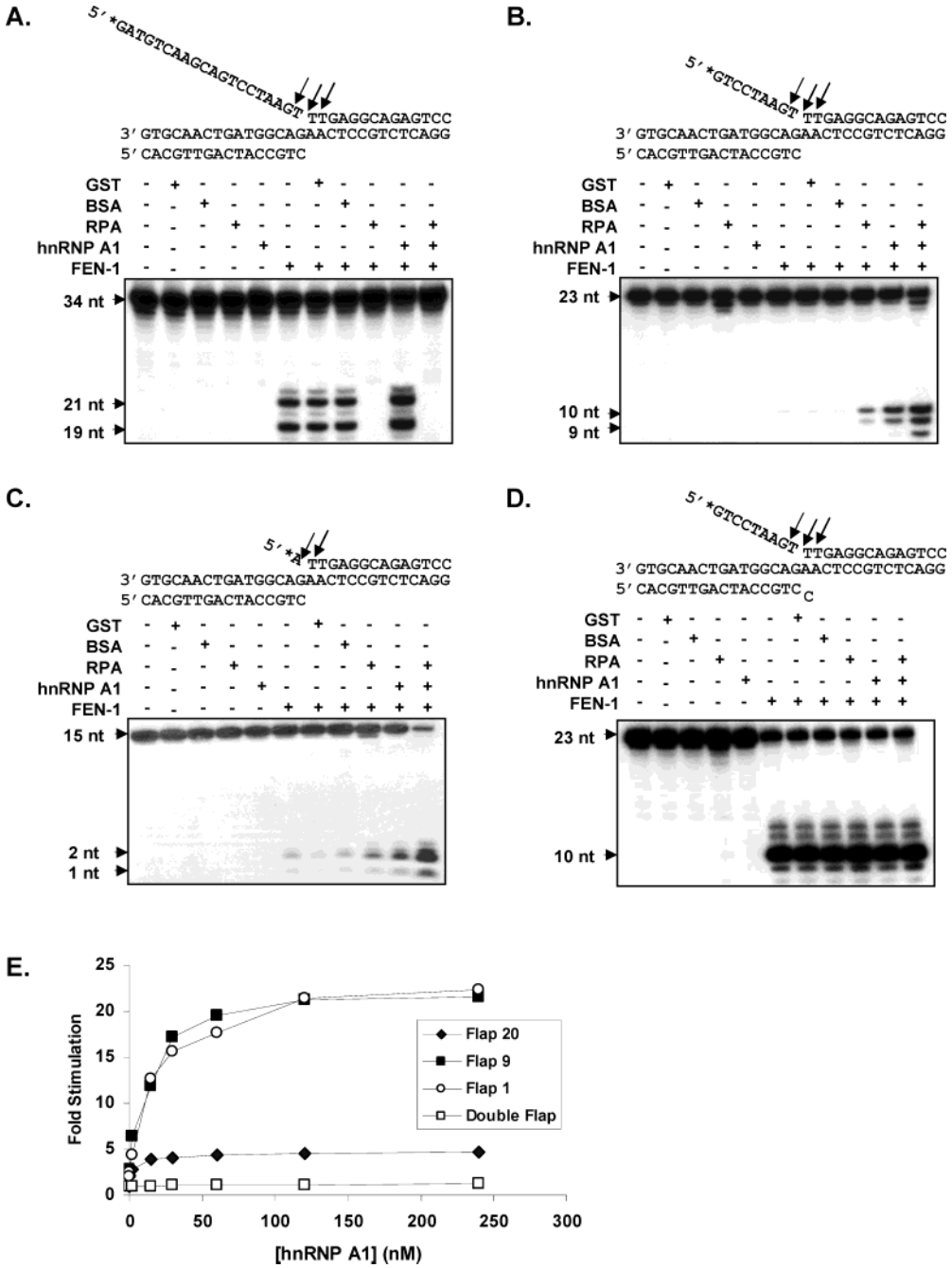

FIGURE 3: hnRNP A1 stimulates nuclease activities of hFEN-1. The effect of hnRNP A1 on hFEN-1 to cleave DNA flap substrates flap 20, flap 9, and flap 1 were determined. hFEN-1 (15 nM) was incubated with flap DNA substrate in the presence of 60 nM GST, BSA, RPA, or hnRNP A1. The DNA substrates and the cleavage products were separated by 15% denaturing PAGE and visualized by autoradiography. (A) Cleavage of the flap 20 substrate (3B1:flap20:G1) by hFEN-1. The 34 nt band represents the noncleaved substrate, and 21 nt and 19 nt bands are the products. (B) Cleavage of the flap 9 substrate (3B1:flap9:G1) by FEN-1. The 23 nt band represents the noncleaved substrate, and 10 nt and 9 nt bands are the products. (C) Cleavage of the flap 1 substrate (3B1:flap1:G1) by FEN-1. The 15 nt band represents the noncleaved substrate, and 1 nt and 2 nt bands are the products. (D) Cleavage of the double-flap DNA substrate (3B2:flap9:G1) by FEN-1. The 23 nt band represents the noncleaved substrate, and the 10 nt band is the major product. (E) hnRNP A1-concentration-dependent cleavage of flap 20, flap 9, and flap 1 substrates by FEN-1 The cleavage of flap 20, flap 9, flap 1, and double-flap DNA substrates by FEN-1 was assayed in the presence of 0, 0.015 0.15, 1.5, 15, 30, 60, 120, and 240 nM hnRNP A1. The nuclease activities were quantified by the IPLab Gel program (Signal Analytics Corp., Vienna, VA). Th fold of stimulation was measured by comparing FEN-1 activity in the presence of hnRNP A1 with FEN-1 activity without hnRNP A1 at each point of hnRNP A1 concentration.

we set out to determine the mechanism of stimulation. One possibility is that the FEN-1/hnRNP A1 complex displays a greater affinity for the DNA substrate than does hFEN-1 alone. A previously published flap DNA substrate binding assay (*27*) was employed to evaluate the effect of hnRNP A1 on the interaction between hFEN-1 and the flap 9 DNA substrate. The results presented in Figure 4 demonstrate that in fact hnRNP A1 does enhance substrate binding by hFEN-1 and the enhancement occurs in an hnRNP A1-concentration-dependent manner. The stimulation is saturated at 120 nM hnRNP A1 with a maximal level of stimulation of approximately 4-fold (Figure 4). The kinetic parameters of FEN-1 in the presence and absence of hnRNP A1 were determined. At 37 °C, in the absence of hnRNP A1, the K_m

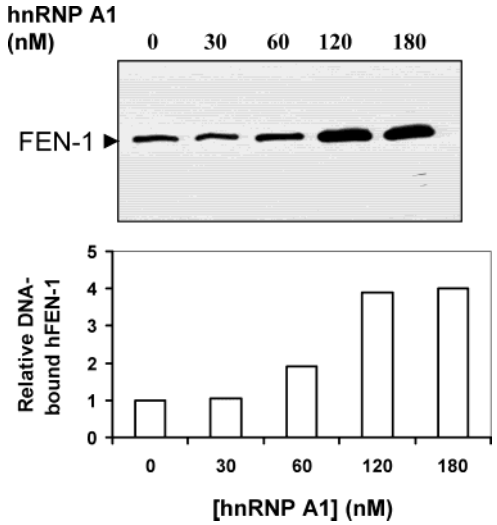

FIGURE 4: hnRNP A1 enhances DNA substrate binding by hFEN-1. Agarose-bound flap 9 DNA substrate (approximately 27 pmol) was incubated with 9 pmol of purified hFEN-1 in the presence of 0, 0.9, 1.8, 3.6, and 5.4 pmol of hnRNP A1. After extensive washing, hFEN-1 bound to the flap 9 substrate was resolved by 4−15% gradient SDS−PAGE and detected by Western blot using polyclonal anti-hFEN-1 antibody. The protein bands in the upper panel were quantified using the IPLab Gel program. The amount of hFEN-1 bound to flap 9 in the absence of hnRNP A1 was arbitrarily set as 1, and relative amounts of hFEN-1 bound to flap 9 in the presence of varying amounts of hnRNP A1 were calculated.

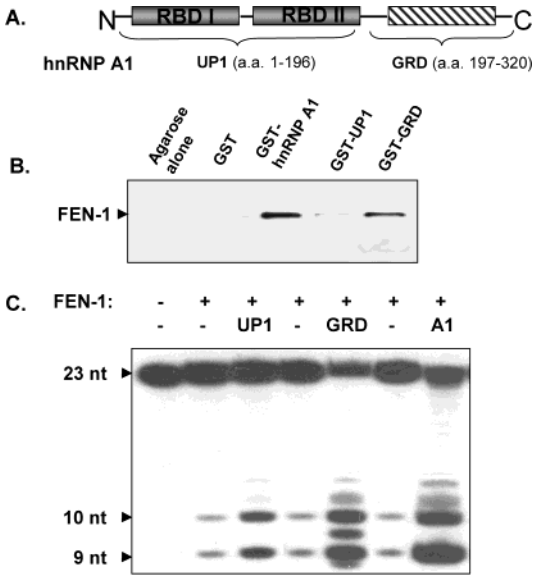

FIGURE 5: The glycine-rich domain is essential for interaction with hFEN-1 but not required for stimulation. (A) Schematic graph of the domain structure of hnRNP A1. The functional domains UP1 and GRD were defined according to a previous study (*30*). The full-length hnRNP A1, UP1, and GRD domain were GST tagged for interaction and nuclease activity stimulation studies. (B) Interaction between hFEN-1 and hnRNP A1 and its mutants. Agarose beads or GST-fusion-protein-bound agarose beads were incubated with cell lysates containing hFEN-1. After washing, the agarose-bound hFEN-1 was analyzed by 4−15% gradient SDS−PAGE followed by Western blot using polyclonal anti-hFEN-1 antibody. (C) Stimulation of FEN-1 activity by hnRNP A1 and its deletion mutants. hFEN-1 (30 nM) was incubated with flap DNA substrate in the presence of 60 nM GST, UP1, GRD, or hnRNP A1. The cleavage products were analyzed as previously described.

and k_{cat} of hFEN-1 were found to be 686 nM and 2 min^{-1}, respectively, while in the presence of hnRNP A1, the K_m and k_{cat} of hFEN-1 were 366 nM and 7 min^{-1}. Thus, inclusion of hnRNP A1 in the reaction decreases K_m by 47%, which is consistent with the DNA binding data presented in Figure 4. Interestingly, hnRNP A1 increases the k_{cat} by 3.5-fold. This indicates that the complex may alter the active site of FEN-1 to allow for more efficient hydrolysis of the phosphodiester bond of the flap substrates. Alternatively, hnRNP A1 may alter the DNA substrate structure to permit more favorable binding and/or catalysis. The combined effects of hnRNP A1 on the substrate binding and catalysis by hFEN-1 result in a total stimulation of flap 9 cleavage activity of approximately 20-fold.

The C-Terminal Glycine-Rich Domain of hnRNP A1 Is Essential for Interaction with hFEN-1 but Not for Stimulation. On the basis of the amino acid sequence of hnRNP A1, two major structural and functional modules have been identified: the N-terminal region of 196 amino acid residues, consisting of two tandemly arranged RNA binding domains (UP1) and a C-terminal auxiliary domain (from 197 to 320 amino acids) rich in glycine (GRD) (*31*). UP1 contributes most of the protein's affinity for RNA (*32*), while GRD plays an important role in protein−protein interactions (*28*). To determine which motifs are critical for interaction and stimulation of FEN-1, we made two truncation mutants of hnRNP A1, GST−UP1 consisting of the first 196 amino acids comprising the RNA binding domain, fused to an N-terminal GST tag, and GST−GRD consisting of amino acids 197−320 comprising the glycine-rich domain fused to an N-terminal GST tag (Figure 5A; *31*). The interaction between hFEN-1 and the two hnRNP A1 truncation mutants was characterized by GST pull-down assays. The results revealed that both intact hnRNP A1 and the C-terminal GRD could efficiently bind hFEN-1 (Figure 5B). In contrast, the N-terminal UP1 was not able to bind to hFEN-1 anymore. The stimulation of hFEN-1 by hnRNP A1 mutants was evaluated by nuclease assay using flap 9 as a DNA substrate. Interestingly, both the truncation mutants GST−UP1 and GST−GRD were able to stimulate hFEN-1 activity (Figure 5C). However, the level of GST−GRD stimulation of hFEN-1 is similar to that observed for the intact hnRNP A1 protein, while GST−UP1 stimulation of hFEN-1 activity was significantly reduced.

DISCUSSION

hnRNP A1 is a multifunctional nuclear protein that was first characterized as a major component of ribonucleoprotein complexes present in the nuclei of mammalian cells (*33*) and is involved in many aspects of RNA metabolism, including RNA splicing (*21*) and nucleocytoplasmic transport of mRNA (*23*, *34*). hnRNP A1 has also been shown to bind to telomere DNA, thus stabilizing and protecting telomere ends from degradation (*22*). The involvement of hnRNP A1 in the regulation of viral RNA processing of human immunodeficiency virus (*35*), human cytomegalovirus (*36*), and human T-cell leukemia virus 2 (*37*) has also been suggested. The identification of the hFEN-1/hnRNP A1 complex suggests that hnRNP A1 might also function in FEN-1-involved DNA metabolism pathways. In mammalian cells, the major function of FEN-1 is to process α-segments during Okazaki fragment maturation. Yeast strains deficient in FEN-1 display replication-error phenotypes, such as a

duplication mutator. Homozygous knockout of FEN-1 in mice is embryonic lethal (*38*). The fact that hnRNP A1 forms a complex with hFEN-1 during the S-phase suggests that hnRNP A1 may play a direct role in DNA replication. There is evidence that FEN-1 participates in base-excision repair (*39*, *40*) and nonhomologous-end-joining pathways (*41*). hnRNP A1 may also be involved in these pathways as an effector of hFEN-1.

The recent model for eukaryotic Okazaki fragment maturation indicated that FEN-1 removes a short DNA flap, which is formed after the Dna2/RPA complex cleaves the major portion of the α-segment (*16*). Our in vitro biochemical assay revealed that FEN-1 was inefficient in processing DNA substrates with the short-flap structure. This property was first identified by Bambara's group in their study on stimulation of FEN-1 by PCNA (*20*). However, in the earlier study by Lieber's group, FEN-1 cleavage efficiency was independent of the flap length. The assay conditions may account for this discrepancy. As in Bambara's work (*20*) and in this work, FEN-1 was assayed in the presence of 40 mM KCl and 50 mM NaCl, respectively, while in the work published by Lieber's group (*42*), FEN-1 activity was assayed in the absence of salt. To determine if FEN-1-length-dependent activity could be attributed to different reaction conditions and ionic strength, cleavage of flap 20, flap 9, and flap 1 DNA substrates by FEN-1 was examined in the absence of salt. The results demonstrated that, under such conditions, FEN-1 efficiently cleaved all three DNA substrates equally well (data not shown). However, salt is present in physiological conditions, where the in vivo reactions take place.

The strong stimulation of hFEN-1 by hnRNP A1 in cleavage of short-flap DNA substrates suggests that hnRNP A1 may work as an accessory factor of FEN-1 to facilitate its function in processing the residual α-segment under the relatively high ionic strength conditions present in the cell. Previous studies by the Seo group (*17*) and our present studies both suggest that RPA is the central regulator in guiding the sequential actions of Dna2 and hFEN-1 in processing the α-segment. RPA first forms a stable complex with the single-stranded RNA−DNA primer. This RPA−DNA interaction stimulates Dna2 activity but inhibits FEN-1, even though it complexes with hnRNP A1. After the cleavage of the RNA−DNA primer by Dna2, the RPA/Dna2 complex dissociates from the short-flap DNA, and enables the FEN-1/hnRNP A1 complex to efficiently remove the remaining DNA portion of the α-segment (Figure 6).

Besides hnRNP A1 and RPA, other eukaryotic proteins, including PCNA (*43*), APE-1 (*44*), DNA polymerase α (*45*) and β (*46*), WRN (*47*), and Dna2 (*15*) have previously been reported to physically or functionally interact with FEN-1. Why does FEN-1 have so many partners? One explanation is that FEN-1 is a multifunctional protein which interacts with proteins of many different DNA metabolism pathways. In DNA replication, FEN-1 may complex with PCNA (*48*), RPA, and the newly identified hnRNP A1. In the base-excision repair pathway, FEN-1 forms a complex with APE-1, Pol β, and PCNA. The FEN-1/WRN complex may play a critical role in the NHEJ DNA repair pathway as both proteins are reported to be required for its function (*41*, *49*, *50*).

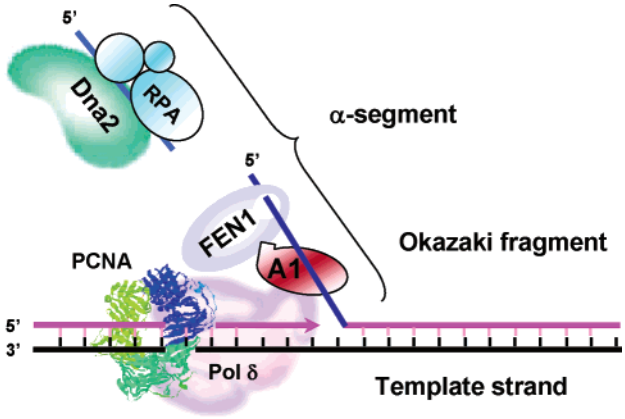

FIGURE 6: Schematic graph of the sequential model of Dna2- and FEN-1-mediated α-segment processing during Okazaki fragment maturation. The formation and processing of the α-segment are represented. Proteins, including Pol δ, PCNA, Dna2, RPA, FEN-1, and hnRNP A1, are displayed. For simplicity, other factors involved in Okazaki fragment maturation are not shown. The direction of the Okazaki fragment extension by Pol δ is indicated by the arrow.

hnRNP A1 physically interacts with hFEN-1 and significantly stimulates the cleavage of the short-flap DNA substrate. The crystal structure of the UP1 domain reveals that the RNA binding clefts of hnRNP A1 are shallow. Docking of a model substrate suggests that hnRNP A1 would be readily accessible to other proteins (*51*). The C-terminal GRD domain is positively charged, a feature that may be used for protein−protein interactions. As an RNA/DNA metabolism accessory protein, hnRNP A1 can interact with either single-stranded RNA or single-stranded DNA. We demonstrated that the interaction between hnRNP A1 and hFEN-1 is mediated through the C-terminal glycine-rich motif of hnRNP A1. Our present data suggest that hnRNP A1 may stimulate hFEN-1 nuclease activity through two different mechanisms, (i) enhancing substrate binding and (ii) increasing catalytic efficiency. By interaction with single-stranded flap DNA, hnRNP A1 can stabilize and present the DNA substrate to hFEN-1, thus facilitating flap strand recognition by hFEN-1. This may be the reason GST−UP1, in which the C-terminal glycine-rich domain of hnRNP A1 is truncated, could still stimulate FEN-1 nuclease activity, regardless of the loss of the interaction site with FEN-1. Moreover, hnRNP A1 may recruit and activate hFEN-1 through protein−protein interaction, thus increasing the catalytic efficiency. Thus, the two stimulation mechanisms might be independent. In further studies, it would be interesting to specify the interaction and stimulation domain as well as how hRNP A1 stimulates FEN-1 nuclease activities.

One puzzle is that hnRNP A1 can stimulate hFEN-1 to cleave flap 20, flap 9, and flap 1, while RPA inhibits hFEN-1 to cleave flap 20 but stimulates the enzyme to cleave flap 9 and flap 1. One possible explanation is that RPA has two distinct binding modes of interaction with single-stranded DNA: RPA forms a stable complex with single-stranded DNA of length greater than 10 nucleotides, but forms an unstable complex with single-stranded DNA of length at 8−10 nucleotides, which is the minimum length for interaction (52). The stable interaction between RPA and the flap strand of the flap 20 substrate prevents hFEN-1 from

accessing the DNA flap. However, the unstable interaction between RPA and the flap DNA of flap 9 substrates creates no barrier for FEN-1, when hFEN-1 binds to the flap strand. Similarly, given that hnRNP A1 forms an unstable complex with the flap DNA substrate, upon recruiting hFEN-1, hnRNP A1 may either move with FEN-1 along the flap strand or dissociate from the flap DNA, thus facilitating the reaction of FEN-1 nuclease. Multiprotein complexes constitute a tightly associated network, which allows accurate and efficient α-segment processing. The development of a reconstitution assay including all players of lagging strand synthesis would help to elucidate the mechanisms of Okazaki fragment maturation.

ACKNOWLEDGMENT

We gratefully thank Dr. Gideon Dreyfuss for providing hnRNP A1 antibody. We also thank Dr. Xinwei Li, Dr. Junzhuan Qiu, Dr. Steve Alas, Steven Bates, and other members in Shen's laboratory for technical assistance and critical reading of the manuscript. We thank Dr. Steve Patrick for purification of RPA.

REFERENCES

1. Hubscher, U., and Seo, Y. S. (2001) *Mol. Cells 12*, 149−157.
2. Jin, Y. H., Ayyagari, R., Resnick, M. A., Gordenin, D. A., and Burgers, P. M. (2003) *J. Biol. Chem. 278*, 1626−1633.
3. MacNeill, S. A. (2001) *Curr. Biol. 11*, R842−R844.
4. Waga, S., and Stillman, B. (1998) *Annu. Rev. Biochem. 67*, 721−751.
5. Bambara, R. A., Murante, R. S., and Henricksen, L. A. (1997) *J. Biol. Chem. 272*, 4647−4650.
6. Qiu, J., Qian, Y., Frank, P., Wintersberger, U., and Shen, B. (1999) *Mol. Cell. Biol. 19*, 8361−8371.
7. Turchi, J. J., Huang, L., Murante, R. S., Kim, Y., and Bambara, R. A. (1994) *Proc. Natl. Acad. Sci. U.S.A. 91*, 9803−9807.
8. Frank, P., Braunshofer-Reiter, C., Wintersberger, U., Grimm, R., and Busen, W. (1998) *Proc. Natl. Acad. Sci. U.S.A. 95*, 12872−12877.
9. Johnson, R. E., Kovvali, G. K., Prakash, L., and Prakash, S. (1995) *Science 269*, 238−240.
10. Reagan, M. S., Pittenger, C., Siede, W., and Friedberg, E. C. (1995) *J. Bacteriol. 177*, 364−371.
11. Sommers, C. H., Miller, E. J., Dujon, B., Prakash, S., and Prakash, L. (1995) *J. Biol. Chem. 270*, 4193−4196.
12. Tishkoff, D. X., Filosi, N., Gaida, G. M., and Kolodner, R. D. (1997) *Cell 88*, 253−263.
13. Lee, K. H., Kim, D. W., Bae, S. H., Kim, J. A., Ryu, G. H., Kwon, Y. N., Kim, K. A., Koo, H. S., and Seo, Y. S. (2000) *Nucleic Acids Res. 28*, 2873−2881.
14. Kang, H. Y., Choi, E., Bae, S. H., Lee, K. H., Gim, B. S., Kim, H. D., Park, C., MacNeill, S. A., and Seo, Y. S. (2000) *Genetics 155*, 1055−1067.
15. Budd, M. E., and Campbell, J. L. (1997) *Mol. Cell. Biol. 17*, 2136−2142.
16. Bae, S. H., Bae, K. H., Kim, J. A., and Seo, Y. S. (2001) *Nature 412*, 456−461.
17. Bae, S. H., and Seo, Y. S. (2000) *J. Biol. Chem. 275*, 38022−38031.
18. Ayyagari, R., Gomes, X. V., Gordenin, D. A., and Burgers, P. M. (2003) *J. Biol. Chem. 278*, 1618−1625.
19. Negritto, M. C., Qiu, J., Ratay, D. O., Shen, B., and Bailis, A. M. (2001) *Mol. Cell. Biol. 21*, 2349−2358.
20. Tom, S., Henricksen, L. A., and Bambara, R. A. (2000) *J. Biol. Chem. 275*, 10498−10505.
21. Biamonti, G., Buvoli, M., Bassi, M. T., Morandi, C., Cobianchi, F., and Riva, S. (1989) *J. Mol. Biol. 207*, 491−503.
22. LaBranche, H., Dupuis, S., Ben-David, Y., Bani, M. R., Wellinger, R. J., and Chabot, B. (1998) *Nat. Genet. 19*, 199−202.
23. Michael, W. M., Choi, M., and Dreyfuss, G. (1995) *Cell 83*, 415−422.
24. Qiu, J., Li, X., Frank, G., and Shen, B. (2001) *J. Biol. Chem. 276*, 4901−4908.
25. Frank, G., Qiu, J., Zheng, L., and Shen, B. (2001) *J. Biol. Chem. 276*, 36295−36302.
26. Patrick, S. M., and Turchi, J. J. (2001) *J. Biol. Chem. 276*, 22630−22637.
27. Gomes, X. V., and Burgers, P. M. (2000) *EMBO J. 19*, 3811−3821.
28. Cartegni, L., Maconi, M., Morandi, E., Cobianchi, F., Riva, S., and Biamonti, G. (1996) *J. Mol. Biol. 259*, 337−348.
29. Biswas, E. E., Zhu, F. X., and Biswas, S. B. (1997) *Biochemistry 36*, 5955−5962.
30. Kao, H. I., Henricksen, L. A., Liu, Y., and Bambara, R. A. (2002) *J. Biol. Chem. 277*, 14379−14389.
31. Mayeda, A., Munroe, S. H., Caceres, J. F., and Krainer, A. R. (1994) *EMBO J. 13*, 5483−5495.
32. Nadler, S. G., Merrill, B. M., Roberts, W. J., Keating, K. M., Lisbin, M. J., Barnett, S. F., Wilson, S. H., and Williams, K. R. (1991) *Biochemistry 30*, 2968−2976.
33. Dreyfuss, G., Matunis, M. J., Pinol-Roma, S., and Burd, C. G. (1993) *Annu. Rev. Biochem. 62*, 289−321.
34. Pinol-Roma, S., and Dreyfuss, G. (1992) *Nature 355*, 730−732.
35. Black, A. C., Luo, J., Chun, S., Bakker, A., Fraser, J. K., and Rosenblatt, J. D. (1996) *Virus Genes 12*, 275−285.
36. Wang, Y. F., Chen, S. C., Wu, F. Y., and Wu, C. W. (1997) *Biochem. Biophys. Res. Commun. 232*, 590−594.
37. Zhang, X., Li, H. P., Xue, W., and Lai, M. M. (1999) *Virology 264*, 115−124.
38. Kucherlapati, M., Yang, K., Kuraguchi, M., Zhao, J., Lia, M., Heyer, J., Kane, M. F., Fan, K., Russell, R., Brown, A. M., Kneitz, B., Edelmann, W., Kolodner, R. D., Lipkin, M., and Kucherlapati, R. (2002) *Proc. Natl. Acad. of Sci. U.S.A. 99*, 9924−9929.
39. Klungland, A., and Lindahl, T. (1997) *EMBO J. 16*, 3341−3348.
40. Ranalli, T. A., Tom, S., and Bambara, R. A. (2002) *J. Biol. Chem. 277*, 41715−41724.
41. Wu, X., Wilson, T. E., and Lieber, M. R. (1999) *Proc. Natl. Acad. Sci. U.S.A. 96*, 1303−1308.
42. Harrington, J. J., and Lieber, M. R. (1994) *EMBO J. 13*, 1235−1246.
43. Li, X., Li, J., Harrington, J., Lieber, M. R., and Burgers, P. M. (1995) *J. Biol. Chem. 270*, 22109−22112.
44. Dianova, II, Bohr, V. A., and Dianov, G. L. (2001) *Biochemistry 40*, 12639−12644.
45. Zhu, F. X., Biswas, E. E., and Biswas, S. B. (1997) *Biochemistry 36*, 5947−5954.
46. Prasad, R., Dianov, G. L., Bohr, V. A., and Wilson, S. H. (2000) *J. Biol. Chem. 275*, 4460−4466.
47. Brosh, R. M., Jr., von Kobbe, C., Sommers, J. A., Karmakar, P., Opresko, P. L., Piotrowski, J., Dianova, I., Dianov, G. L., and Bohr, V. A. (2001) *EMBO J. 20*, 5791−5801.
48. Gary, R., Park, M. S., Nolan, J. P., Cornelius, H. L., Kozyreva, O. G., Tran, H. T., Lobachev, K. S., Resnick, M. A., and Gordenin, D. A. (1999) *Mol. Cell. Biol. 19*, 5373−5382.
49. Cooper, M. P., Machwe, A., Orren, D. K., Brosh, R. M., Ramsden, D., and Bohr, V. A. (2000) *Genes Dev. 14*, 907−912.
50. Oshima, J., Huang, S., Pae, C., Campisi, J., and Schiestl, R. H. (2002) *Cancer Res. 62*, 547−551.
51. Ding, J., Hayashi, M. K., Zhang, Y., Manche, L., Krainer, A. R., and Xu, R. M. (1999) *Genes Dev. 13*, 1102−1115.
52. Blackwell, L. J., and Borowiec, J. A. (1994) *Mol. Cell. Biol. 14*, 3993−4001.

BI035364T